

University of Bucharest - Faculty of Physics

**Defect states in some selected würtzite
semiconductors by an *ab initio* method**

Master's Dissertation

Author:

Adela NICOLAEV

Coordinators:

Conf. Dr. Lucian ION

Dr. Alexandru G. NEMNES

Bucharest - June 2010

Contents

| | | |
|----------|--|-----------|
| 1 | Introduction | 2 |
| 2 | Density functional theory | 3 |
| 2.1 | The Hohenberg-Kohn Theorems | 3 |
| 2.2 | The Kohn-Sham Formulation | 5 |
| 3 | Pseudopotential | 8 |
| 3.1 | The Pseudopotential Approximation | 8 |
| 3.2 | Norm Conserving Pseudopotential | 10 |
| 3.3 | Kleinman-Bylander Pseudopotentials | 11 |
| 3.4 | Step by step pseudopotential generation | 11 |
| 4 | Defects | 14 |
| 4.1 | Definition of point defects | 14 |
| 4.2 | Geometrical Configuration of Point Defects | 15 |
| 4.2.1 | The Vacancy | 15 |
| 4.2.2 | The divacancy | 16 |
| 4.2.3 | The interstitial | 16 |
| 4.2.4 | Complex Defects | 18 |
| 4.2.5 | Aggregates | 18 |
| 4.3 | Lattice Distortion and Relaxation | 19 |
| 5 | DFT calculae in crystalline systems | 20 |
| 5.1 | Basis Set | 21 |
| 5.2 | Electron Hamiltonian | 22 |
| 5.3 | Sampling the Brillouin Zone | 22 |
| 6 | Results | 24 |
| 6.1 | Bulk | 24 |
| 6.2 | Vacancies | 28 |
| 6.3 | Impurities | 31 |
| 6.4 | Complex defects | 33 |
| 7 | Conclusions | 37 |
| 8 | Personal thanks | 38 |

Chapter 1

Introduction

During the past few decades as well as in the present days, the microelectronics crucially depends on the control over impurity doping and structural defects in semiconductors. Since in the process of doping point defects may appear, it is essential to know how they affect the energy spectrum of host material.

Point defects can be of several types:

- substitutional impurities with non-isovalent neighbors who may become donor or acceptor; depending on their position inside the band gap, one can further classify them into shallow or deep donors (acceptors).

- isovalent impurities which may have capture state and which pattern life time of nonequilibrium carriers

- vacancies and interstitial dopants (intrinsic defects) which may be of the same nature as material atoms or different. These, although they may have a strong doping character are thermally unstable and is technologically inefficient.

In this work we studied vacancies, like V_N in aluminium nitride and V_B in boron nitride, substitutional impurities, such as aluminium nitride doped with germanium and boron nitride doped with carbon, and complex defects in these two structures.

In order to find the differences in the band structure, between the ideal bulk systems and the ones mentioned above, we employ DFT (Density Functional theory) calculations in a super-cell framework. As numerical method to be used in this work we have chosen SIESTA (Spanish Initiative for Electronic Simulations with Thousands of Atoms), which has the major advantage that it scales linearly with the number of atoms.

Chapter 2

Density functional theory

Density functional theory is a theory of correlated many-body systems. It is included here in close association with independent-particle methods, because it has provided the key step that has made possible development of practical, useful independent-particle approaches that incorporate effects of interactions and correlations among the particles. As such, density functional theory has become the primary tool for calculation of electronic structure in condensed matter, and is increasing important for quantitative studies of molecules and other finite systems. The remarkable successes of the approximate local density (LDA) and generalized-gradient approximation (GGA) functionals within the Kohn-Sham approach have led to widespread interest in density functional theory as the most promising approach for accurate, practical methods in the theory of materials. The original density functional theory of quantum systems is the method of Thomas and Fermi proposed in 1927. Although their approximation is not accurate enough for present-day electronic structure calculations, the approach illustrates the way density functional theory works. In the original Thomas-Fermi method the kinetic energy of the system electrons is approximated as an explicit functional of density, idealized as non-interacting electrons in a homogeneous gas with density equal to the local density at any given point. Both Thomas and Fermi neglected exchange and correlation among the electrons; however, this was extended by Dirac in 1930, who formulated the local approximation for exchange still in use today.

The attraction of density functional theory is evident by the fact that one equation for the density is remarkably simpler than the full many-body Schrodinger equation that involves $3N$ degrees of freedom for N electrons. The Thomas-Fermi type approach has been applied to equations of state of the elements. However, the Thomas-Fermi-type approach starts with approximations that are too crude, missing essential physics and chemistry, such as shell structures of atoms and binding of molecules. DFT was put on a firm theoretical footing by the two Hohenberg-Kohn theorems. [2]

2.1 The Hohenberg-Kohn Theorems

The Hohenberg-Kohn theorems relate to any system consisting of electrons moving under the influence of an external potential $v_{ext}(r)$. Stated simply they are as follows:

Theorem 1

The external potential $v_{ext}(r)$, and hence the total energy, is a unique functional of the electron density $n(r)$.

The energy functional $E[n(r)]$ alluded to in the first Hohenberg-Kohn theorem can be written in terms of the external potential $v_{ext}(r)$ in the following way

$$E[n(r)] = \int n(r)v_{ext}(r)dr + F[n(r)], \quad (2.1)$$

where $F[n(r)]$ is an unknown, but otherwise universal functional of the electron density $n(r)$ only. Correspondingly, a Hamiltonian for the system can be written such that the electron wavefunction ψ that minimizes the expectation value gives the groundstate energy (assuming a non-degenerate groundstate)

$$E[n(r)] = \langle \psi | \hat{H} | \psi \rangle \quad (2.2)$$

The Hamiltonian can be written as

$$\hat{H} = \hat{F} + \hat{V}_{ext} \quad (2.3)$$

where \hat{F} is the electronic Hamiltonian consisting of a kinetic energy operator \hat{T} and an interaction operator \hat{V}_{ee}

$$\hat{F} = \hat{T} + \hat{V}_{ee} \quad (2.4)$$

The electron operator F is the same for all N-electrons systems, so H is completely defined by the number of electrons N , and the external potential $v_{ext}(r)$.

The proof of the first theorem is remarkably simple and proceeds by reductio ad absurdum. Let there be two different external potentials, $v_{ext,1}(r)$ and $v_{ext,2}(r)$, that give rise to the same density $n_0(r)$. The associated Hamiltonians, \hat{H}_1 and \hat{H}_2 , will therefore have different groundstate wavefunctions, ψ_1 and ψ_2 , that each yield $n_0(r)$. Using the variational principle, together with Eqs. 2.3 and 2.4, yields

$$E_1^0 < \langle \psi_2 | \hat{H}_1 | \psi_2 \rangle < \langle \psi_2 | \hat{H}_2 | \psi_2 \rangle + \langle \psi_2 | \hat{H}_1 - \hat{H}_2 | \psi_2 \rangle = E_2^0 + \int n_0(r) |v_{ext,1}(r) - v_{ext,2}(r)| dr \quad (2.5)$$

where E_1^0 and E_2^0 are the groundstate energies of \hat{H}_1 and \hat{H}_2 respectively. It is at this point that the Hohenberg-Kohn theorems, and therefore DFT, apply rigorously to the groundstate only. An equivalent expression for Eq. 2.5 holds when the subscript are interchanged. Therefore adding the interchanged inequality to Eq. 2.5 leads to the result:

$$E_1^0 + E_2^0 < E_2^0 + E_1^0 \quad (2.6)$$

results in which is a contradiction, and as a result the groundstate density uniquely determines the external potential $v_{ext}(r)$, to within an additive constant. Stated simply, the electrons determine the positions of the nuclei in a system, and also all groundstate electronic properties, because as mentioned earlier, $v_{ext}(r)$ and N completely define \hat{H} .

Theorem 2

The groundstate energy can be obtained variationally: the density that minimizes the total energy is the exact groundstate density.

The proof of the second theorem is also straightforward: as just shown, $n(r)$ determines $v_{ext}(r)$ determine \hat{H} and therefore ψ .

This ultimately means ψ is a functional of $n(r)$, and so the expectation value of \hat{F} is also a functional of $n(r)$, i.e.

$$F[n(r)] = \langle \psi | \hat{F} | \psi \rangle$$

A density that is the ground-state of some external potential is known as v -representable. Following from this, a v -representable energy functional $E_v[n(r)]$ can be defined in which the external potential $v(r)$ is unrelated

to another density $n'(r)$,

$$E_v|n(r)| = \int n'(r)v_{ext}(r)dr + F|n'(r)|$$

and the variational principle asserts

$$\langle \psi' | \hat{F} | \psi' \rangle + \langle \psi' | \hat{V}_{ext} | \psi' \rangle > \langle \psi | \hat{F} | \psi \rangle + \langle \psi | \hat{V}_{ext} | \psi \rangle$$

where ψ is the wavefunction associated with the correct groundstate $n(r)$. This leads to

$$\int n'(r)v_{ext}(r)dr + F|n'(r)| > \int n(r)v_{ext}(r)dr + F|n(r)|$$

and so the variational principle of the second Hohenberg-Kohn theorem is obtained,

$$E_v|n'(r)| > E_v|n(r)|$$

Although the Hohenberg-Kohn theorems are extremely powerful, they do not offer a way of computing the ground-state density of a system in practice.

2.2 The Kohn-Sham Formulation

Within the framework of Kohn-Sham DFT, the intractable many body problem of interacting electrons in a static external potential is reduced to a tractable problem of non-interacting electrons moving in an effective potential. The effective potential includes the external potential and the effects of the Coulomb interactions between the electrons, the exchange and correlation interactions. Modelling the latter two interactions comes the difficulty within KS DFT. The simplest approximation is the local-density approximation(LDA), which is based upon exact exchange energy for a uniform electron gas, which can be obtained from the Thomas-Fermi model, and from fits to the correlation energy for a uniform electron gas. Non-interacting systems are relatively easy to solve as the wave function can be represented as a Slater determinant of orbitals. Further, the kinetic energy functional of such a system is known exactly. The exchange-correlation part of the total-energy functional remains unknown and must be approximated. [2]

The Kohn-Sham approach is to replace the difficult interacting many-body system obeying the Hamiltonian with a different auxiliary system that can be solved more easily. Since there is no unique prescription for choosing the simpler auxiliary system, this is an ansatz that replace the issues. The ansatz of Kohn and Sham assumes that the ground state density of the original interacting system is equal to that of some chosen non-interacting system. This leads to independent-particle equations for the non-interacting system that can be considered exactly soluble with all the difficult many-body terms incorporated into an exchange-correlation functional of the density. By solving the equations one finds the ground state density and energy of the original interacting system with the accuracy limited only by the approximations in the exchange-correlation functional. Here we will consider the Kohn-Sham ansatz for the ground state, which is by far the most widespread way in which the theory has been applied. The fundamental theorems of density functional theory show that in principle the ground state density determines everything. [1]

The Kohn-Sham ansatz rests upon two assumptions:

1. The exact ground state density can be represented by the ground state density of an auxiliary system of non-interacting particles. This is called “non-interacting-V- representability”, although there are no rigorous

proofs for real system of interest, we will proceed assuming its validity. This leads to the relation of the actual and auxiliary system shown in Fig.2.1

2.The auxiliary Hamiltonian is chosen to have the usual kinetic operator and an effective local potential $V_{eff}^\sigma(r)$ acting on an electron of spin σ at point r . The local form is not essential[1], but it is an extremely useful simplification that is often taken as the defining characteristic of the KS approach. We assume that the external potential V_{ext} is spin independent[2]; nevertheless, except in cases that are spin symmetric, the auxiliary effective potential $V_{eff}^\sigma(r)$ must depend upon spin in order give the correct density for each spin.

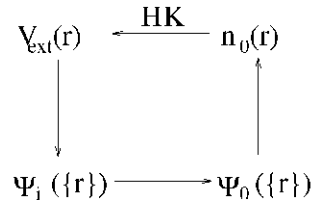


Figure 2.1: Schematic representation of KS ansatz. The notation HK_0 denotes the Hohenberg-Kohn theorem applied to the non-interacting problem. The arrow labeled KS provides the connection in both directions between the many-body and independent-particle systems, so that the arrows connect any point to any other point. Therefore, in principle, solution of the independent-particle Kohn-Sham problem determines all properties of the full many-body system.

The actual calculations are performed on the auxiliary independent-particle system defined by the auxiliary Hamiltonian (using Hartree atomic units $\hbar = m_e = e = \frac{4\pi\epsilon_0}{1}$)

$$H_{aux}^\sigma = -\frac{1}{2}\nabla^2 + V^\sigma(r)$$

At this point the form of $V^\sigma(r)$ is not specified and the expressions must apply for all $V^\sigma(r)$ in some range, in order to define functionals for a range of densities. For a system of $N = N^\uparrow + N^\downarrow$ independent electrons obeying this Hamiltonian, the ground state has one electron in each of the N^σ orbitals $\psi_i^\sigma(r)$ with the lowest eigenvalues ϵ_i^σ of the Hamiltonian [1]. The density of the auxiliary system is given by sums of squares of the orbitals for each spin

$$n(r) = \sum_\sigma n(r, \sigma) = \sum_\sigma \sum_{i=1}^{N^\sigma} |\psi_i^\sigma(r)|^2$$

the independent-particle kinetic energy T_s is given by

$$T_s = -\frac{1}{2} \sum_\sigma \sum_{i=1}^{N^\sigma} \langle \psi_i^\sigma | \nabla^2 | \psi_i^\sigma \rangle = \frac{1}{2} \sum_\sigma \sum_{i=1}^{N^\sigma} |\nabla \psi_i^\sigma|^2,$$

and we define the classical Coulomb interaction energy of the electron density $n(r)$ interacting with itself

$$E_{Hartree}[n] = \frac{1}{2} \int d^3r d^3r' \frac{n(r)n(r')}{|r-r'|}$$

The Kohn-Sham approach to the full interacting many-body problem is to rewrite the Hohenberg-Kohn expression for the ground state energy functional in the form

$$E_{KS} = T_s[n] + \int dr V_{ext}(r)n(r) + E_{Hartree}[n] + E_{ii} + E_{xc}[n]$$

Here $V_{ext}(r)$ is the external potential due to the nuclei and any another external fields (assumed to be independent of spin) and E_{ii} is the interaction between the nuclei. Thus the sum of the terms involving $V_{ext}, E_{Hartree}$ and E_{ii} forms a neutral grouping that is well defined. The independent-particle kinetic energy T_s is given explicitly as a functional of the orbitals; however, T_s for each spin σ must be a unique functional of the density $n(r, \sigma)$ by application of the Hohenberg-Kohn arguments applied to the independent-particle Hamiltonian [1]

All many-body effects of exchange and correlation are grouped into the exchange-correlation energy E_{xc} . Comparing the Hohenberg-Kohn and Kohn-Sham expressions for the total energy shows that E_{xc} can be written in terms of the Hohenberg-Kohn functional as

$$E_{xc}[n] = E_{HK}[n] - (T_s[n] + E_{Hartree}[n]),$$

or in the revealing form

$$E_{xc}[n] = \langle \hat{T} \rangle - T_s[n] + \langle \hat{V}_{int} \rangle - E_{Hartree}[n].$$

Here $[n]$ denotes a functional of the density $n(r, \sigma)$ which depends upon both position in space r and spin σ . One can see that $E_{xc}[n]$ must be a functional since the right-hand sides of the equations are functionals. The latter equation shows explicitly that E_{xc} is just the difference of the kinetic and internal interaction energies of the true interacting many-body system from those of the fictitious independent-particle system with electron-electron interactions replaced by the Hartree energy.[1]

If the universal functional $E_{xc}[n]$ defined in the last equation, were known, then the exact ground state energy and density of the many-body electron problem could be found by solving the Kohn-Sham equations for independent-particles. To the extent that an approximate form for $E_{xc}[n]$ describes the true exchange-correlation energy, the Kohn-Sham method provides a feasible approach to calculating the ground state properties of the many-body electron system.

Chapter 3

Pseudopotential

The pseudopotential is an attempt to replace the complicated effects of the motion of the core electrons of an atom and its nucleus with an effective potential, or pseudopotential, so that the Schrodinger equation contains a modified effective potential term instead of the Coulombic potential term for core electrons normally found in the Schrodinger equation. The pseudopotential approximation was first introduced by Hans Hellman in the 1930s. By construction of this pseudopotential, the valence wavefunction generated is also guaranteed to be orthogonal to all core states.

The pseudopotential is an effective potential constructed to replace the atomic all-electron potential such that core states are eliminated and the valence electrons are described by nodeless pseudo-wavefunctions. In this approach only the chemically active valence electrons are dealt with explicitly, while the core electrons are “frozen”, being considered together with the nuclei as rigid non-polarizable ion cores. Norm-conserving pseudopotentials are derived from an atomic reference state, requiring that the pseudo- and all-electron valence eigenstates have the same energies and amplitude (and thus density) outside a chosen core cutoff radius r_c . Pseudopotentials with larger cutoff radius are said to be softer, that is more rapidly convergent, but at the same time less transferable, that is less accurate to reproduce realistic features in different environments.

Motivation:

1. Reduction of basis set size
2. Reduction of number of electrons
3. Inclusion of relativistic and other effects

Approximation:

1. One-electron picture.
2. Small core approximation assumes that there is no significant overlap between core and valence WF. So the exchange correlation potential is:

$$E_{xc}(n_{core} | n_{valence}) = E_{xc}(n_{core}) + E_{xc}(n_{valence})$$

3.1 The Pseudopotential Approximation

It has been shown by the use of Bloch’s theorem, that a plane wave energy cut-off in the Fourier expansion of the wavefunction and careful k-point sampling that the solution to the Kohn-Sham equations for infinite crystalline systems is now tractable. Unfortunately a plane wave basis set is usually very poorly suited to expanding the electronic wavefunctions because a very large number are required to accurately describe the rapidly oscillating wavefunctions of electrons in the core region.

and pseudopotential are identical to the all electron wavefunction and potential outside a radius cut-off r_c . This condition has to be carefully checked for as it is possible for the pseudopotential to introduce new non-physical states (so called ghost states) into the calculation.

The pseudopotential is also constructed such that the scattering properties of the pseudo wavefunction are identical to the scattering properties of the ion and core electrons. In general, this will be different for each angular momentum dependence are called non-local pseudopotentials.

The usual methods of pseudopotential generation firstly determine the all electron eigenvalues of an atom using the Schrodinger equation:

$$\left\{ -\frac{\hbar^2}{2m} \nabla^2 + V \right\} \psi_{AE_l}$$

where ψ_{AE_l} is the wavefunction for the all electron (AE) atomic system with angular momentum component l . The resulting valence eigenvalues are substituted back into Schrodinger equation but with a parametrized pseudo wavefunction function of the form.

$$\psi_{ps_l} = \sum_{i=1}^n \alpha_i j_l$$

Here, j_l are spherical Bessel functions. The coefficients, α_i , are the parameters fitted to the conditions listed below. In general the pseudo wave function is expanded in three or four spherical Bessel functions.

The pseudopotential is then constructed by directly inverting the Kohn-Sham equation with the pseudo wavefunction ψ_{ps_l} .

A pseudopotential is not unique, therefore several methods of generation also exist. However they must obey several criteria. These are:

1. The core charge produced by the pseudo wavefunction must be the same as that produced by the atomic wavefunction. This ensures that the pseudo atom produces the same scattering properties as the ionic core.
2. Pseudo-electron eigenvalues must be the same as the valence eigenvalues obtained from the atomic wavefunctions.
3. Pseudo wavefunctions must be continuous at the core radius as well as its first and second derivative and also be non-oscillatory.
4. On inversion of the all electron Schrodinger equation for the atom, excited states may also be included in the calculation (if appropriate for a given condensed matter problem), for example, generating a d component for a non-local pseudopotential when the ground state of an atom does not contain these angular momentum components.

3.2 Norm Conserving Pseudopotential

To obtain the exchange-correlation energy accurately it is necessary that outside the core region the real and pseudo wavefunctions be identical so that both wavefunction generate identical charge densities. Generation of a pseudopotential that satisfies

$$\int_0^{r_c} \psi_{AE}^*(r) \psi_{AE}(r) dr = \int_0^{r_c} \psi_{ps}^*(r) \psi_{ps}(r) dr$$

where $\psi_{AE}^*(r)$ is the electron wavefunction and $\psi_{ps}^*(r)$ is the pseudo wavefunction, guarantees the equal-

ity of the all electron and pseudo wavefunctions outside the core region. In practice this is achieved using a non-local pseudopotential which uses a different potential for each angular momentum component of the pseudopotential. This also best describes the scattering properties from the ion core.

Pseudopotential of this type are known as non-local norm-conserving pseudopotential and are the most transferable since they are capable of describing the scattering properties of an ion in a variety of atomic environments.[4]

3.3 Kleinman-Bylander Pseudopotentials

The most general form of non-local pseudopotential is

$$V_{ion} = \sum_{lm} |Y_{lm}\rangle V_l \langle Y_{lm}|$$

where Y_{lm} are spherical harmonics and V_l is the l^{th} angular momentum component of the pseudopotential acting on the wavefunction. If there are N_{pw} plane waves in the expansion of the wavefunction at each k-point and there are N_k k-points then the evaluation of V_{ion} will require $N_{pw}N_k(N_{pw} + 1)/2$ projectors of the above form to be calculated for each angular momentum component l .

The crystal potential $V_{cr}(r)$ is obtained by placing a pseudopotential for each species at each site in the lattice. The structure factor incorporates the crystal symmetry, hence

$$V_{cr}(G - G') = \sum_s s_s(G - G') V_{ps}(G - G')$$

where the summation index is over ionic species and the structure factor for each species is $s_s(G - G') = \sum_i \exp(i(G - G')R_i)$. The total ion-electron energy is then

$$E_{elec} = \sum_{ion,lm} \langle \psi | Y_{lm} \rangle V_{cr}(G - G') \langle Y_{lm} | \psi \rangle$$

It can be seen that this gives an inseparable double sum over G and G' . Evaluation of the ion-electron contribution to the total energy therefore scales as the square of the number of plane waves used in the expansion. This is computationally inefficient and will severely limit the size of any calculation.

A more efficient way of evaluating this contribution is due to Kleinman and Bylander. By expressing the pseudopotential in a different form they were able to split the double sum into a product of two single sums. The Kleinman-Bylander pseudopotential has the form

$$V_{ion} = V_{LOC} + \sum \frac{|\psi_{lm}\delta V_l\rangle \langle \delta V_l\psi_{lm}|}{\langle \psi_{lm} | \delta V_l | \psi_{lm} \rangle}$$

where V_{loc} is an arbitrary local potential, ψ_{lm} are pseudo atom wavefunction and δV_l is defined by $\delta V_l = V_{l,NL} - V_{LOC}$, where $V_{l,NL}$ is the l angular momentum component of a non-local pseudopotential.

3.4 Step by step pseudopotential generation

The sequence of processes required to produce a potential is as follows:

1. The KS equations are solved for the atom. It is important to include in the construction all the orbitals that will take part in bonding the solid state.

2. Then, the solution to the all-electron KS equations for the atom produce a set of all-electron wavefunctions and energy levels, which in turn can construct the all electron potential $V^v(r)$. This potential contains the exchange-correlation, Hartree and nuclear potential, and is singular at $r = 0$.

3. From these all-electron quantities, one constructs a first approximation to the pseudopotential for each value of the angular momentum, l .

4. generate all-electron wavefunctions

5. choose the matching radii- r_c is the radius at which the pseudo-wavefunction and true wavefunction approach each other, and is termed the core radius. Care must be taken in the choice of value for r_c since taking too large a value will remove critical bonding information from the potential.

6. choose if we want the core corrections

7. generate the pseudopotential

8. The potential that gives rise to the pseudo-wavefunction is obtained by inverting the Schrodinger using the energy levels of the all-electron system. Such a potential would then give rise to a wavefunction that agrees with the all electron wavefunction outside the core radius, and also generates the all-electron energy levels

9. check its transferability

10. check the required cutoff

11. check its separable form

To generate the pseudopotential that we need later for SIESTA we used another program called "ATOM". The program was originally written in 1982 by Sverre Froyen at the University of California at Berkeley, modified starting in 1990 by Norman Troullier and Jose Luis Martins at the University of Minnesota, and currently maintained by Alberto Garcia.

The program's basic capabilities are:

- All-electron DFT atomic calculations for arbitrary electronic configurations
- Generation of ab-initio pseudopotentials
- Atomic calculations in which the effect of the core is represented by a previously generated pseudopotential. These are useful to make sure that the pseudopotential correctly reproduces the all-electron results for the valance complex.

In the next images are emphasis pseudopotentials obtained by with the "ATOM" program for boron and nitrogen for quantum number $l = 0, 1$. Both potential were generated with LDA exchange-correlation approach.

For both boron and nitride orbitals 2s and 2p are occupied and orbitals from 1s are in core so we neglected them. The cutting radius used was $r_c = 1.71$ Bohrs. The way these graphics are obtained and the reason we need them were explained in this section.

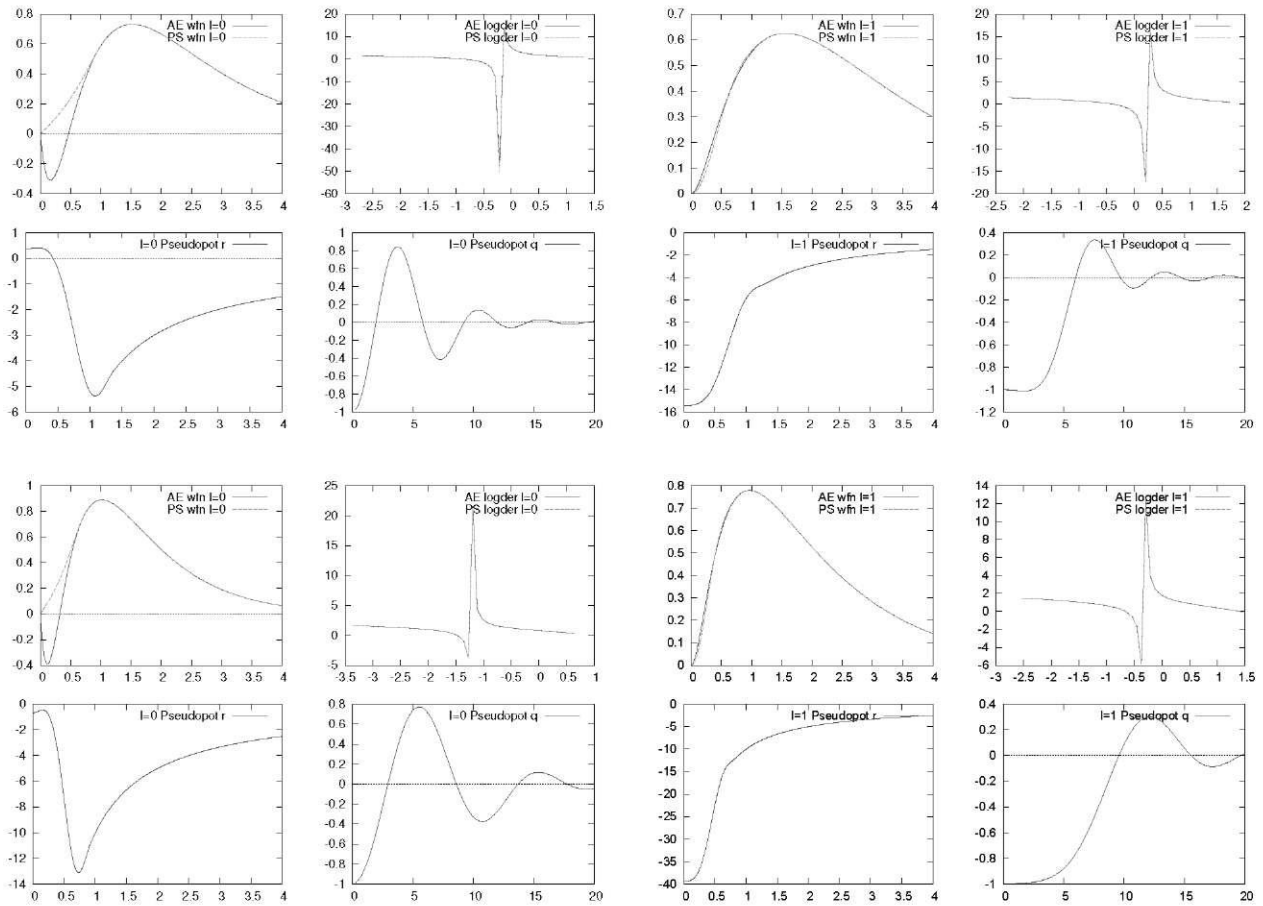


Figure 3.2: a) all electron pseudo-wavefunction-after r_c are identical, b) the logarithmic derivative of the wavefunctions, c) pseudopotential, d) the Fourier transform of the pseudopotential

Chapter 4

Defects

4.1 Definition of point defects

A point defect in a crystal is an entity that causes an interruption in the lattice periodicity. This occurs during the following circumstances.

a) An atom is removed from its regular lattice site; the defect is a vacancy.

b) An atom is in a site different from a regular (substitutional) lattice site; the defect is an interstitial. An interstitial defect can be of the same species as the atoms of the lattice (it is an intrinsic defect, the self-interstitial) or of a different nature (it is then an extrinsic defect, an interstitial impurity).

c) An impurity occupies a substitutional site.

Various kinds of defects are also formed by the association of intrinsic or extrinsic, substitutional or interstitial defects. For instance, a vacancy close to a self-interstitial is a Frenkel pair; two vacancies on neighboring lattice sites form a divacancy. In compound semiconductors all the lattice sites, interstitial as well as substitutional, are not equivalent and a larger variety of intrinsic as well as extrinsic defects exists. For instance, in a 2-6 or 3-5 compound, there are two different sublattices each having its own vacancy, its own interstitial, and its own substitutional or interstitial impurity. An atom of one sublattice placed in the other sublattice forms an “anti-site” defect.[11]

All these various types of defects are schematized in Fig. 4.1. They are “point” defects in contrast to one-dimensional defects (dislocations), two-dimensional defects (surfaces, grain boundaries) or three-dimensional defects (voids, cavities). Small aggregates of several point defects can still be considered as point defects. In that case, the frontier between a point defect and a three-dimensional one is not well defined.[8]

The notion of point defect implies that the perturbation of the lattice remains localized, i.e., it involves an atomic site and few neighbors. But the associated electronic perturbation can extend to larger distances and be, at the limit, delocalized. The above definition of point defects makes reference to a perfect system with translational periodicity which is a result of long-range order. The perfect lattice arrangement is only broken in a localized region. However, the geometrical definition requires only the existence of the same point defects in amorphous covalent materials since, in these materials, the short-range order is preserved. Indeed in amorphous covalent materials, the interatomic distance as well as the bond angle are nearly equal to their counterparts in the crystal. Consequently, the environments of a point defect in both types of materials, because of the distortion and relaxation the defect induces, are qualitatively similar.[9]

Finally, when the concentration of the defects is large enough so that they interact (i.e. there is an overlap of the individual perturbations they induce), they cannot be considered as isolated point defects; defect ordering can occur.

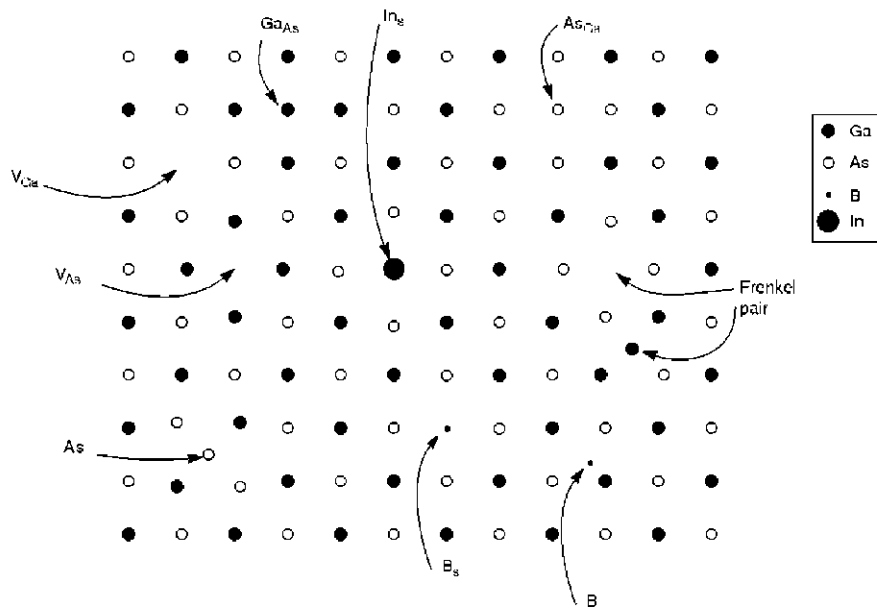


Figure 4.1: Point defects in semiconductors : vacancies, interstitials, Frenkel pairs.

4.2 Geometrical Configuration of Point Defects

4.2.1 The Vacancy

Four bonds are broken in order to remove an atom from its lattice site and form a vacancy (Fig. 4.2a). The broken (dangling) bonds can form new bonds, leading to atomic displacements. This bonding depends on the charge state of the vacancy, i.e., on the number of electrons which occupy these dangling bonds (Fig. 4.2b. and Fig. 4.2c.). The small atomic displacements of the neighbors of the vacancy can be inward or outward displacements that preserve the local symmetry (relaxation) or alter it (distortion). The amplitude of these displacements as well as the new symmetry depend on the type of the bonding, i.e., on the charge state [3],[10].

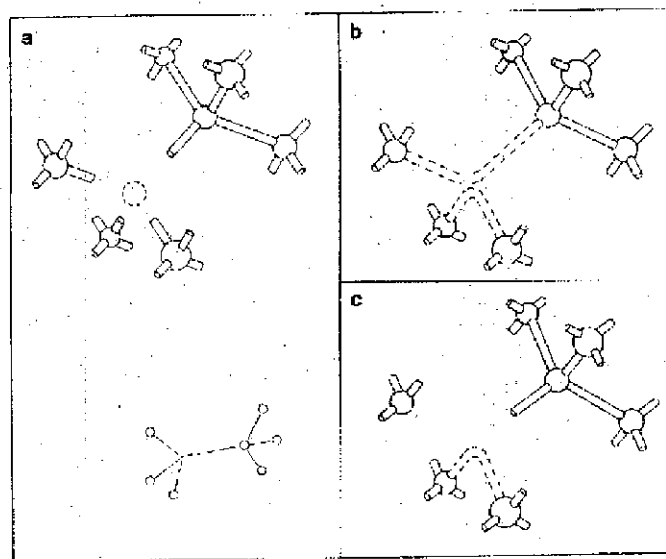


Figure 4.2: The vacancy in diamond lattice and its schematic representation in two dimensions. a) Four bonds are broken in order to create the vacancy. b) When there is one electron per dangling bond they form two new bonds leading to local distortion. c) When an electron is missing one of these two bonds is weakened since it contains only one electron.

4.2.2 The divacancy

The divacancy is formed by the removal of two neighboring atoms Fig. 4.3.. The split-divacancy configuration, corresponding to the configuration of the divacancy in the saddle point for the migration is given in Fig. 4.4. As for the vacancy case, the type of bonding (and hence the distortion and relaxation the neighboring atoms undergo) the dangling bonds form is dependent upon their electronic occupancy[3].

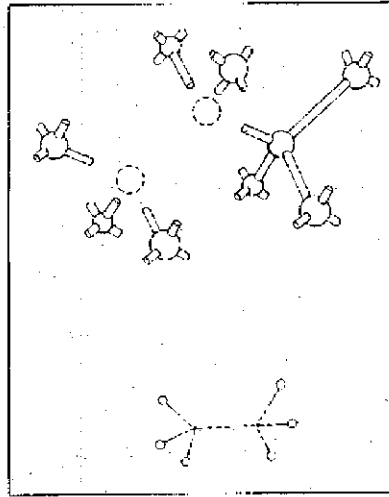


Figure 4.3: The divacancy configuration and its schematic two-dimensional representation

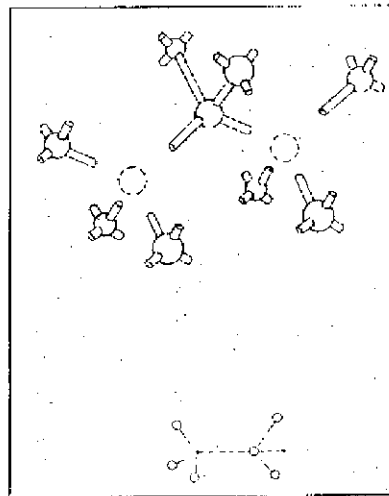


Figure 4.4: The split-divacancy configuration and its schematic two-dimensional representation

4.2.3 The interstitial

It is impossible to decide a priori what are the stable sites for an interstitial atom. However, we can say that in positions of high symmetry, the total electronic energy (with all other atoms at their perfect position) will be an extremum. It is thus reasonable to consider that some of these high-symmetry sites are the stable interstitial positions. Because of the symmetry of the lattice, there may be several equivalent positions per unit cell.

Two neighboring stable interstitial sites are separated by other high-symmetry positions which correspond to saddle points of the electronic energy when all other atoms are again kept fixed at their perfect crystal positions. All these arguments based on the symmetry of the lattice can be altered, for instance, when the electron-phonon interaction is taken into account. This interaction can give rise to distortions of system. As a

result the stable positions will no longer be those of high symmetry. There can be “off-centered” configurations in which the interstitial is slightly displaced from its ideal site. In this respect, once the ideal site has been identified, the situation becomes much the same as for the vacancy [3].

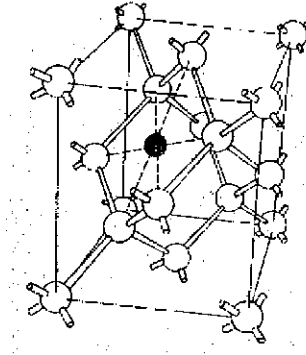


Figure 4.5: The hexagonal interstitial configuration

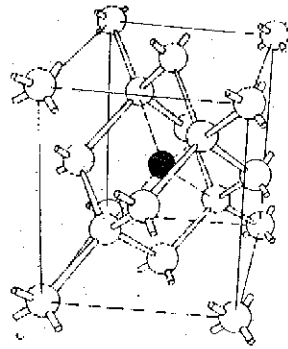


Figure 4.6: The tetrahedral interstitial configuration

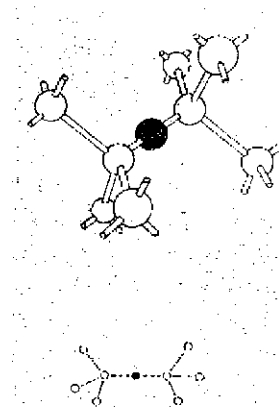


Figure 4.7: The bond-centered interstitial configuration and its schematic two-dimensional representation

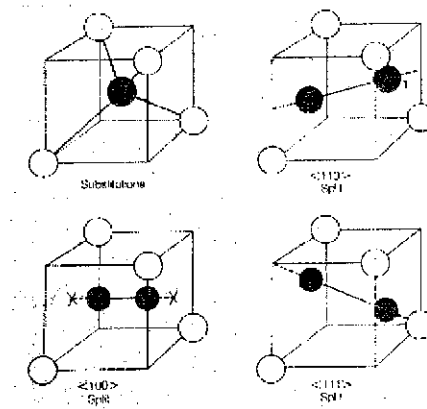


Figure 4.8: Some split-interstitial configurations

4.2.4 Complex Defects

When a simple defect moves, it can interact with other intrinsic as well as extrinsic point defects giving rise to a more complex defect. For instance, when the vacancy becomes mobile in silicon, it can be trapped by an oxygen impurity (present in Czochralski in grown material) and form V - O complex (the A center), or by the doping impurity (Al for instance) and form V-Al complex (the E center), or by another vacancy (in undoped floating zone material) and form divacancies. Fig. 4.9. gives the configuration of the A center in which the oxygen atom occupies a position slightly displaced from the substitutional vacancy site [3].

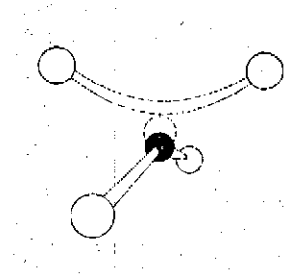


Figure 4.9: In the A-center configuration (vacancy + oxygen complex), the oxygen atom is slightly displaced off the substitutional position

4.2.5 Aggregates

When the concentration of a particular defect is large, they tend to aggregate as the temperature is increased. Vacancies form divacancies that upon becoming mobile or dissociating, form trivacancies, quadrivacancies and so on. In principle, the larger the number of defects involved in an aggregate, the larger the number of possible configurations. But when the number of vacancies in the complex is large, they tend to arrange themselves in lines, rings, or platelets. This behavior should also be true for self-interstitials and for any type of extrinsic defects [3].

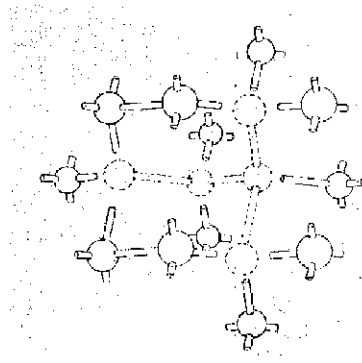


Figure 4.10: One possible configurations for a pentavacancy

4.3 Lattice Distortion and Relaxation

We have already mentioned that the introduction of a point defect induces displacements of the lattice atoms which surround it. The atoms involved are first neighbors, second neighbors, depending on the range of the perturbation introduced by the defect. When the symmetry of the lattice is conserved, these displacements are said to result in a relaxation; when the symmetry is lowered, the induced displacement are said to result in a distortion. The amplitude as well as the type of displacement the lattice atoms undergo is obtained theoretically by minimizing the total energy of the system, lattice plus defect, versus the positions of the various atoms involved in the distortion or in the relaxation. With an increasing number of atoms involved in the distortion, the number of displacements to be considered increases rapidly and the problem becomes quickly impracticable.

The type of distortion depends on the way the defect is bonded to the neighboring atoms. As a result, the distortion is a function of the charge state of the defect. This notion is very important, because it results in a charge-state dependence of energies and entropies. Consequently all the properties which are related to these quantities, defect concentration at thermal equilibrium, stability, migration, diffusion, solubility, vibrational modes, electron-phonon interaction will be charge-state dependent. A manifestation of this charge state dependence of a distortion is Jahn-Teller effect [11].

Chapter 5

DFT calculae in crystalline systems

Siesta is both a method and its computer program implementation, to perform electronic structure calculations and ab initio molecular dynamics simulations of molecules and solids. Its main characteristics are:

- It uses the standard Kohn-Sham self consistent density functional method in the local density (LDA-LSD) or generalized gradient (GGA) approximations.
- It uses norm-conserving pseudopotential in its fully nonlocal (Kleinman-Bylander) form.
- It uses atomic orbitals as basis set, allowing unlimited multiple-zeta and angular momenta, polarization and off-site orbitals. The radial shape of every orbital is numerical and any shape can be used and provided by the user, with the only condition that it has to be of finite support, it has to be strictly zero beyond a user-provided distance from the corresponding nucleus. Finite-support basis sets are the key for calculating the Hamiltonian and overlap matrices in $O(N)$ operations.
- Projects the electron wavefunctions and density onto a real-space grid in order to calculate the Hartee and exchange-correlation potentials and their matrix elements
- Besides the standard Rayleigh-Ritz eigenstate method, it allows the use of localized linear combinations of the occupied orbitals (valence-bond or Wannier-like functions), making the computer time and memory scale linearly with the number of atoms. Simulations with several hundred atoms are feasible with modest workstations.

It routinely provides:

- Total and partial energies
- Atomic forces
- Stress tensor
- Electric dipole moment
- Atomic, orbital and bond populations (Mulliken)
- Electron density

And also (though not all options are compatible):

- Geometry relaxation, fixed or variable cell

- Constant-temperature molecular dynamics (Nose thermostat)
- Variable cell dynamics (Parrinello-Rahman)
- Spin polarized calculations (collinear or not)
- k-sampling of the Brillouin zone
- Local and orbital-projected density of states
- Band structure

5.1 Basis Set

Order- N methods rely heavily on the sparsity of the Hamiltonian and overlap matrices. The sparsity requires either the neglect of matrix elements that are small enough or the use of strictly confined basis orbitals, i.e., orbitals that are zero beyond a certain radius. Within this radius, our atomic basis orbitals are products of a numerical radial functional times a spherical harmonic. For atom I , located at \mathbf{R}_I ,

$$\phi_{lm}(\mathbf{r}) = \phi_{lm}(r_I) Y_{lm}(\hat{\mathbf{r}}_I)$$

where $\mathbf{r}_I = \mathbf{r} - \mathbf{R}_I$, $r = |\mathbf{r}_I|$, and $\hat{\mathbf{r}}_I = \frac{\mathbf{r}_I}{r}$. The angular momentum (labeled by l, m) may be arbitrarily large and, in general, there will be several orbitals (labeled by index n) with the same angular dependence, but different radial dependence, which is conventionally called a “multiple- ζ ” basis. Each radial function may have a different cutoff radius and, up to that radius, its shape is completely free and can be introduced by the user in an input file.

In the case of a minimal (single- ζ) basis set, we have found convenient and efficient the method of Sankey and Niklewski. Their basis orbitals are the eigenfunctions of the (pseudo) atom within a spherical box. In other words, they are the (angular-momentum-dependent) numerical eigenfunctions $\phi_l(r)$ of the atomic pseudopotential $V_l(r)$, for an energy $\epsilon_l + \delta\epsilon_l$ chosen so that the first node occurs at the desired cutoff radius r_l^c :

$$\left(-\frac{1}{2r} \frac{d^2}{dr^2} r + \frac{l(l+1)}{2r^2} + V_l(r)\right) \phi_l(r) = (\epsilon_l + \delta\epsilon_l) \phi_l(r)$$

with $\phi_l(r_l^c) = 0$. In order to obtain a well balanced basis, in which the effect of the confinement is similar for all the orbitals, it is usually better to fix a common “energy shift” $\delta\epsilon$, rather than a common radius r^c , for all the atoms and angular momenta. This means that the orbital radii depend on the atomic species and angular momentum.

One obvious possibility for multiple- ζ bases is to use pseudopotential eigenfunctions with an increasing number of nodes. They have the virtue of being orthogonal and asymptotically complete. The efficiency of this kind of basis depends on the radii of confinement of the different orbitals, since the excited states of the pseudopotential are usually unbound. Another possibility is to use the atomic eigenstates for different ionization states.[4]

The user can feed into Siesta the atomic basis set he/she chooses by means of radial tables, the only limitation being:

- i) the functions have to be atomic-like (radial functions multiplied by spherical harmonics)
- ii) they have to be of finite support, i.e., each orbital becomes strictly zero beyond some cutoff radius chosen by the user.

5.2 Electron Hamiltonian

Within the non-local-pseudopotential approximation, the standard Kohn-Sham one electron Hamiltonian may be written as:

$$\hat{H} = \hat{T} + \sum_I V_I^{local}(r) + \sum_I \hat{V}_I^{KB} + V^H(r) + V^{XC}(r)$$

where $\hat{T} = -\frac{1}{2}\nabla^2$ is the kinetic energy operator, I is an atom index, $V^H(r)$ and $V^{XC}(r)$ are the Hartree and XC potentials, and $V_I^{local}(r)$ and \hat{V}_I^{KB} are the local and non-local (Kleinman-Bylander) parts of the pseudopotential of atom I .

Since the atomic basis orbitals are zero beyond the cutoff radius $r_i^c = \max_l(r_{il}^c)$, the screened “neutral-atom” (NA) potential $V_I^{NA} \equiv V_I^{local} + V_I^{atom}$, is also zero beyond this radius. Now let $\delta\rho(r)$ be the difference between self-consistent electron density $\rho(r)$ and the sum of atomic densities $\rho^{atom} = \sum_l \rho_l^{atom}$, and let $\delta V^H(r)$ be the electrostatic potential generated by $\delta\rho(r)$, which integrates to zero and is usually much smaller than $\rho(r)$. Then the total Hamiltonian may be written as:

$$\hat{H} = \hat{T} + \sum_I V_I^{KB} + \sum_I V_I^{NA}(r) + \delta V^H(r) + V^{xc}(r)$$

The matrix elements of the first two terms involve only two-center integrals which are calculated in reciprocal space and tabulated as a function of interatomic distance. The remaining terms involve potentials which are calculated on a three-dimensional real-space grid.[4]

5.3 Sampling the Brillouin Zone

Brillouin zones are an important characteristic of crystal structure. Integration of all magnitudes over the Brillouin zone (BZ) is essential for small and moderate large unit cells, especially of metals. Although Siesta is designed for large unit cell, in practice it is very useful, especially for comparisons and checks, to be able to also perform calculations efficiently on smaller systems without using expensive superlattices. On the other hand, an efficient k -sampling implementation should not penalize, because of the required complex arithmetic, the Γ -point calculation used in large cells (Fig. 5.1.).

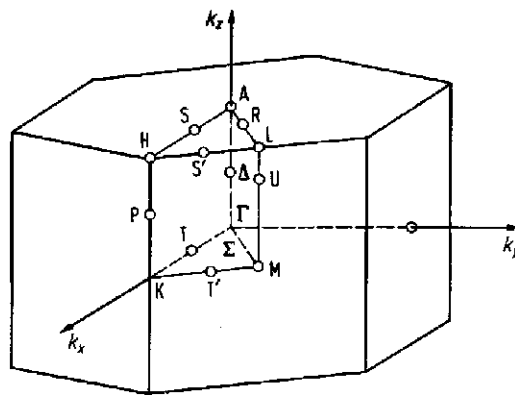


Figure 5.1: Brillouin zone of hexagonal lattice

Around the unit cell we define an auxiliary supercell large enough to contain all the atoms whose basis

orbitals are non-zero at any of the basis orbitals in it. We calculate all the non-zero two-center integrals between the unit cell basis orbitals and the supercell orbitals, without any complex phase factors. We also calculate the grid integrals between all the supercell basis orbitals $\phi_{\mu'}$ and $\phi_{\nu''}$ (primed indices run over all the supercell), but within the unit cell only. We accumulate these integrals in the corresponding matrix elements, thus making use of the relation

$$\langle \phi_{\mu} | V(r) | \phi_{\nu'} \rangle = \sum_{(\mu' \nu'' = \mu \nu')} \langle \phi_{\mu'} | V(r) f(r) | \phi_{\nu''} \rangle$$

$f(r) = 1$ for r within the unit cell and is zero otherwise. Once all the real overlap and Hamiltonian matrix elements are calculated, we multiply them, at every k -point by the corresponding phase factors and accumulate them by folding the supercell orbital to its unit-cell counterpart. Thus

$$H_{\mu\nu}(k) = \sum_{\nu'=v} H_{\mu\nu'} e^{ik(R_{\nu'} - R_{\mu})}$$

The resulting $N \times N$ complex eigenvalue problem, with N the number of orbitals in the unit cell, is then solved at every sampled k point, finding the Bloch-state expansion coefficients $c_{\mu i}(k)$:

$$\psi_i(k, r) = \sum_{\mu'} e^{ikR_{\mu'}} \phi_{\mu'}(r) c_{\mu' i}(k)$$

The electron density is then

$$\rho(r) = \sum_i \int_{BZ} n_i(k) |\psi_i(k, r)|^2 dk = \sum_{\mu' \nu'} \rho_{\mu' \nu'} \phi_{\nu'}^*(r) \phi_{\mu'}(r) \quad (5.1)$$

where the sum is again over all basis orbitals in space and the density matrix

$$\rho_{\mu\nu} = \sum_i \int_{BZ} c_{\mu i}(k) n_i(k) c_{\nu i}(k) e^{ik(R_{\nu} - R_{\mu})} dk \quad (5.2)$$

Thus, to calculate the density at a grid point of the unit cell, we simply find the sum 5.1 over all the pairs of orbitals ϕ_{μ}, ϕ_{ν} in the supercell that are non-zero at that point.

In practice, the integral in 5.2 is performed in a finite, uniform grid of the Brillouin zone. The fineness of this grid is controlled by a k -grid cutoff l_{cut} , a real-space radius which plays a role equivalent to the planewave cutoff of the real-space grid. The origin of the k -grid may be displaced from $k=0$ in order to decrease the number of nonequivalent k -points.

If the unit cell is large enough to allow a Γ -point-only calculation, the multiplication by phase factors is skipped and a single real-matrix eigenvalue problem is solved. In this way, no complex arithmetic penalty occurs, and the differences between Γ -point and k -sampling are limited to a very small section of the code, while all the two-center and grid integrals use always the same real-arithmetic code.[4]

Chapter 6

Results

The starting point in this study was the crystalline system with the crystallographic constants, subsequently allowing the structural relaxation.

First we calculated the corresponding position for atoms in an elementary wurtzite cell, then these were shifted on the three axes in order to produce a “triple” cell with a volume 27 times bigger than the elementary cell. In the middle of the cell were placed different types of defects (Fig. 6.1) and using the Born von Karman conditions, we construct the infinite super-crystal formed by these super-cells.

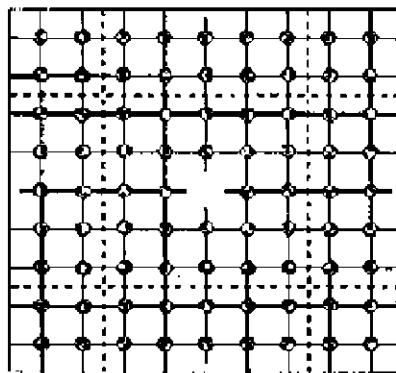


Figure 6.1: super-cell with one defect

The bigger super-cell reproduces more accurately the positioning of the associated energy level of the defect, limiting its splitting in a band. Because a bigger cell demands a larger computational amount of time one has to reach a compromise between these two elements.

6.1 Bulk

First of all we will study the bulk case for the two systems, aluminium nitride (Fig. 6.2) and boron nitride (Fig. 6.3).

Aluminium nitride (AlN) is a semiconductor with a large direct gap. Since it crystallizes in wurtzite lattice the band structure differs from that of the most other III-IV compounds [5]. To check out the pseudopotential we obtained the density of states and energy dispersion, which have been plotted for the bulk system (Fig. 6.2.). We can observe that the band gap is a direct one.

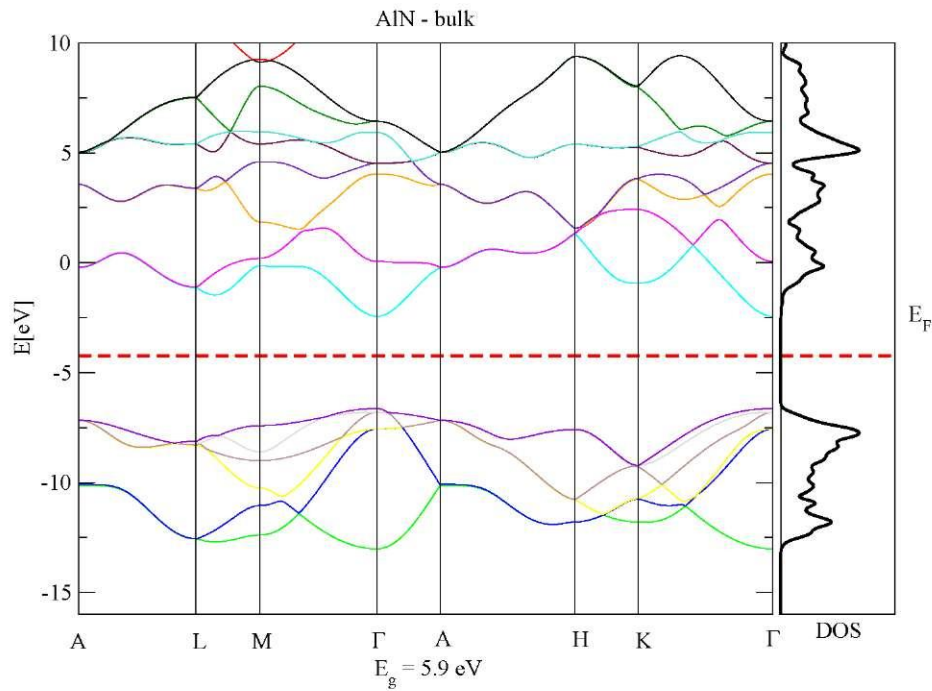


Figure 6.2: Band structure and density of states for Aluminium nitride

Boron nitride (BN) is a chemical compound which is not found in nature and is therefore produced synthetically from boron acid and boron trioxide. The initial product is amorphous BN powder, which is converted to crystalline h-BN by heating in nitrogen flow at temperatures above 1500°C . Wurtzite BN can be obtained via statistic high-pressure or dynamic shock methods. The limit of its stability are not well defined.[6][7] We plotted the density of states and energy dispersion for boron nitride bulk also in Fig (6.3.), but in this case we found, as expected an indirect band gap.

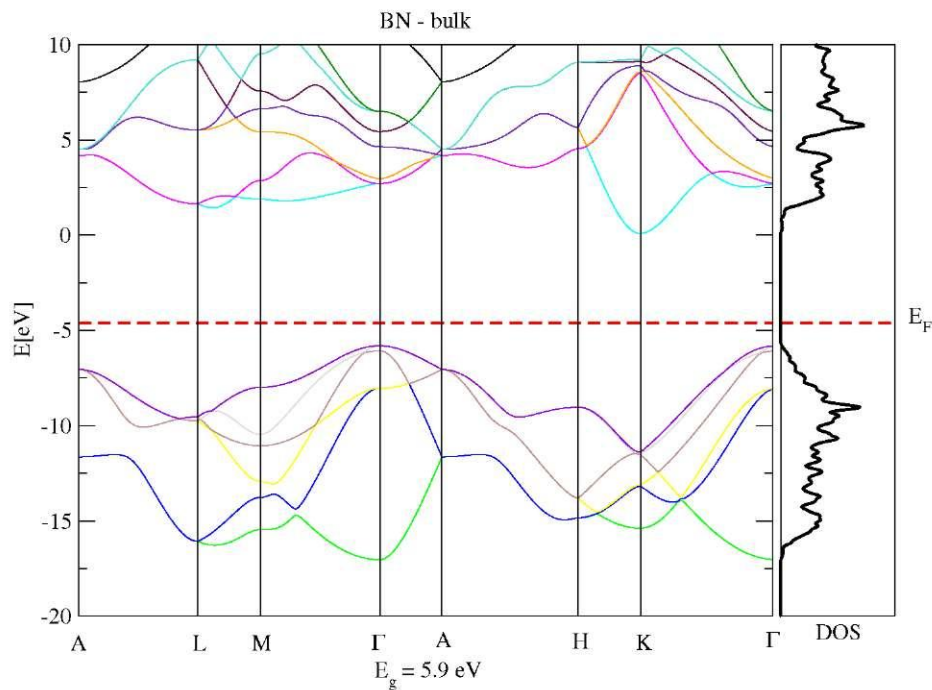


Figure 6.3: Band structures and density of states for Boron nitride

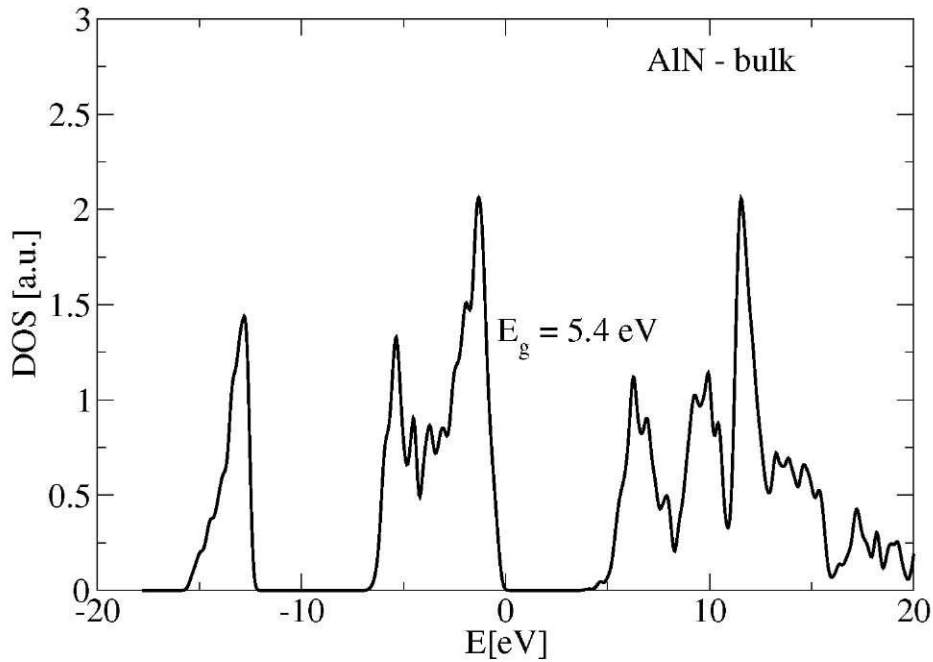


Figure 6.4: Density of states for aluminium nitride bulk

In the case of aluminium nitride we obtained a value for the band gap of 5.4 eV which is close to the experimental one which has a value of 5.8 eV. The Fermi level is positioned at, and Fermi level has the value $E_F = -4.8\text{eV}$.

One can see in Fig.6.5 that for aluminium nitride the edge of valence band is given by 2p orbitals of nitrogen, while the 2s orbitals from nitrogen and 2s orbitals from aluminium form the states from the edge of conduction band. That is why we can state that the band gap for AlN bulk is a direct one and transitions are allowed between valence and conduction band.

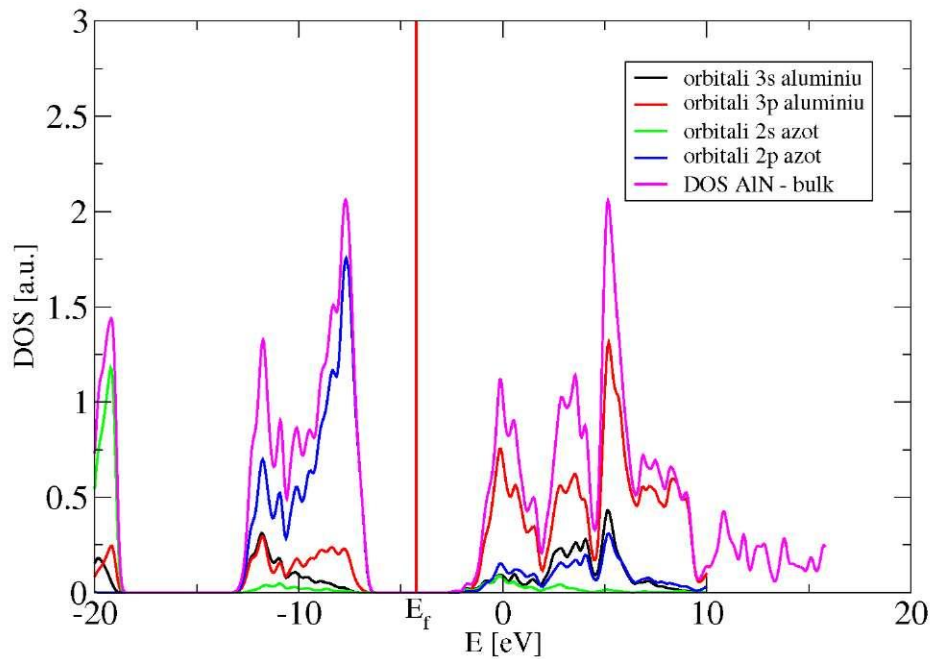


Figure 6.5: Partial DOS for aluminium nitride

For bulk boron nitride Fig. 6.6 the band gap obtained is 5.9 eV, while the experimental value is 6.2 eV, and

Fermi level is $E_F = -3.4\text{eV}$.

For boron nitride Fig. 6.7, the edge of valence band is given by 2p orbitals of nitrogen and by 2p orbitals of boron. The conduction band is given by 2p orbitals from nitrogen and 2p orbitals from boron. In this case the transition between bands are not allowed, and in order for them to occur they have to be mediated by phonon scattering.

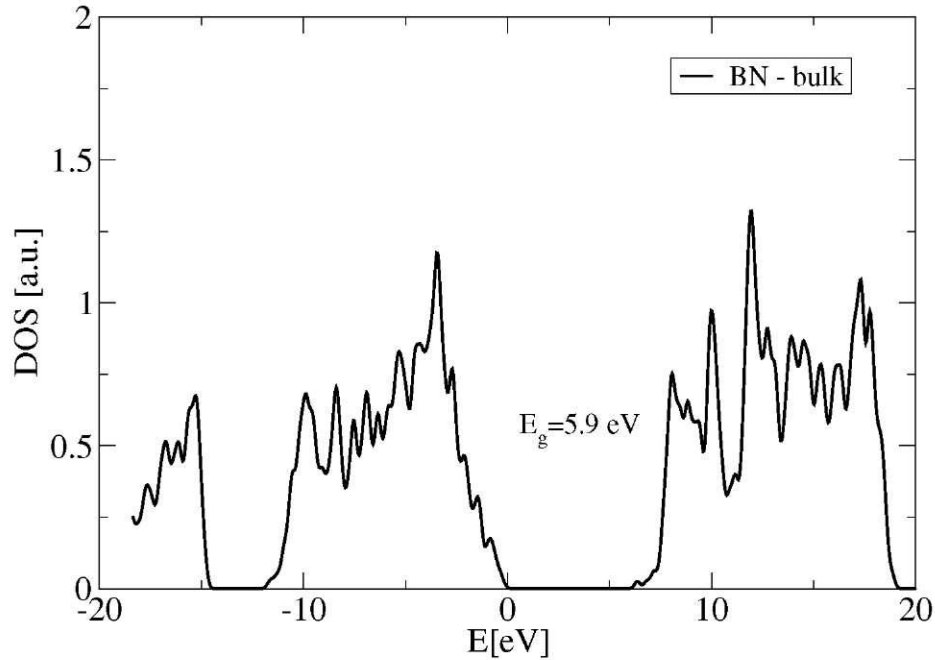


Figure 6.6: Density of states boron nitride bulk

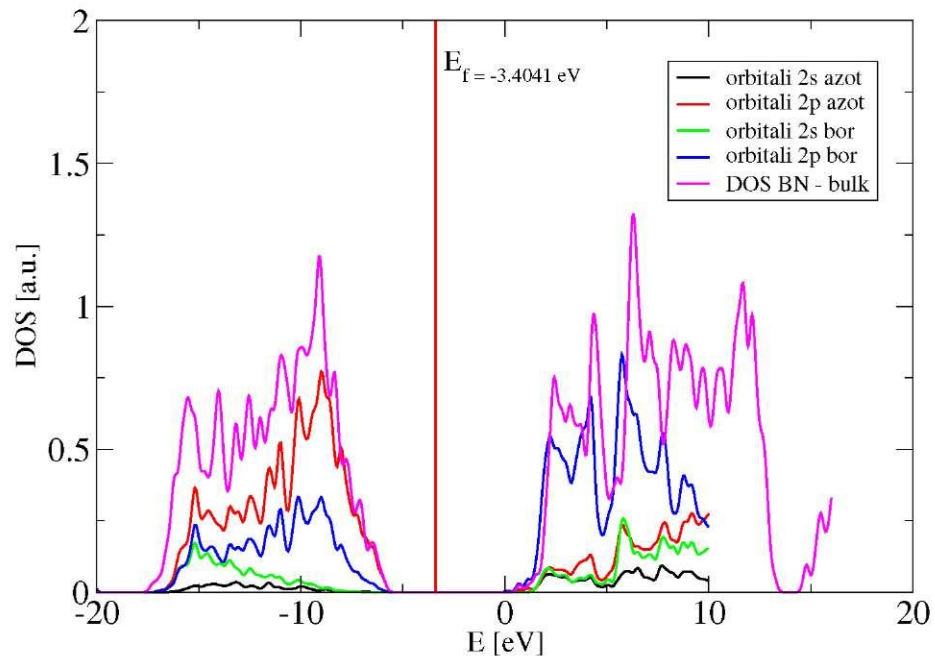


Figure 6.7: Partial DOS for boron nitride bulk

We notice that for bulk structure relaxation did not lead to a significant change of lattice parameters. (Fig. 6.8)

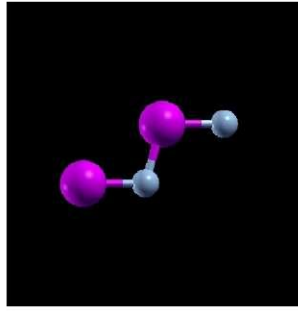


Figure 6.8: Bulk-after relaxation

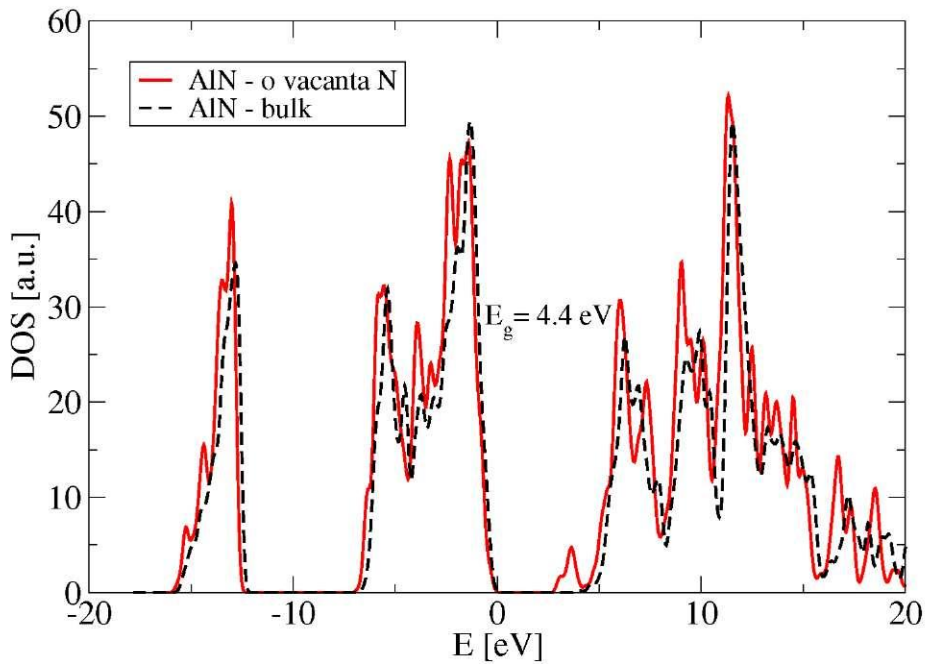
6.2 Vacancies

In Fig. 6.9 we observe the influence of defect V_N in conduction band, resulting in a new split in band.

For the case of nitrogen vacancy (V_N) in aluminium nitride the states from the valence band are given mostly by nitrogen's orbitals and less by aluminium orbitals, while the states from conduction band are given mainly by the latter. New edge states appear in conduction band because of defect V_N .

The vacancy leads to the appearance of o group of states with a donor character, which are mainly formed by nitrogen orbitals.

The value for band gap is $E_g = 4.4\text{eV}$, which is effectively decreased by the presence of the donor levels near the conduction band.

Figure 6.9: Density of states: V_N in aluminium nitride

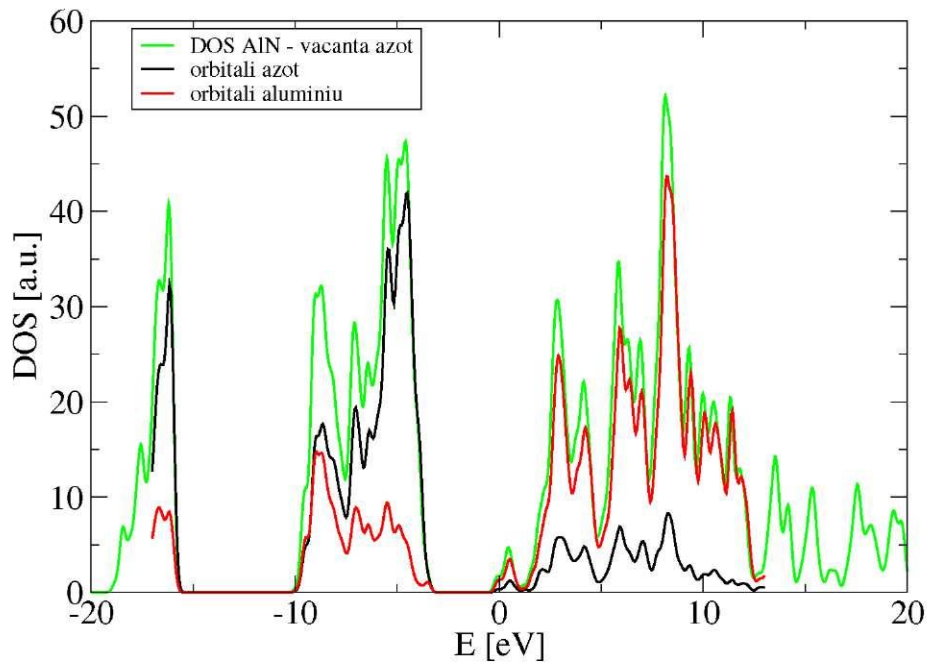


Figure 6.10: Partial DOS for V_N in aluminium nitride

In Fig. 6.11 we can see the influence of a similar defect in the AlN structure.

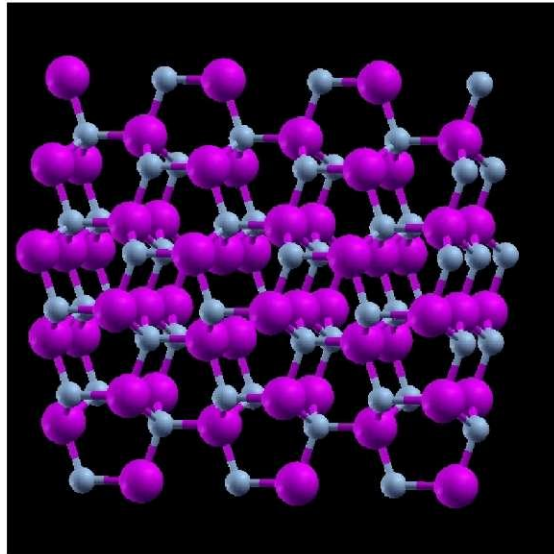
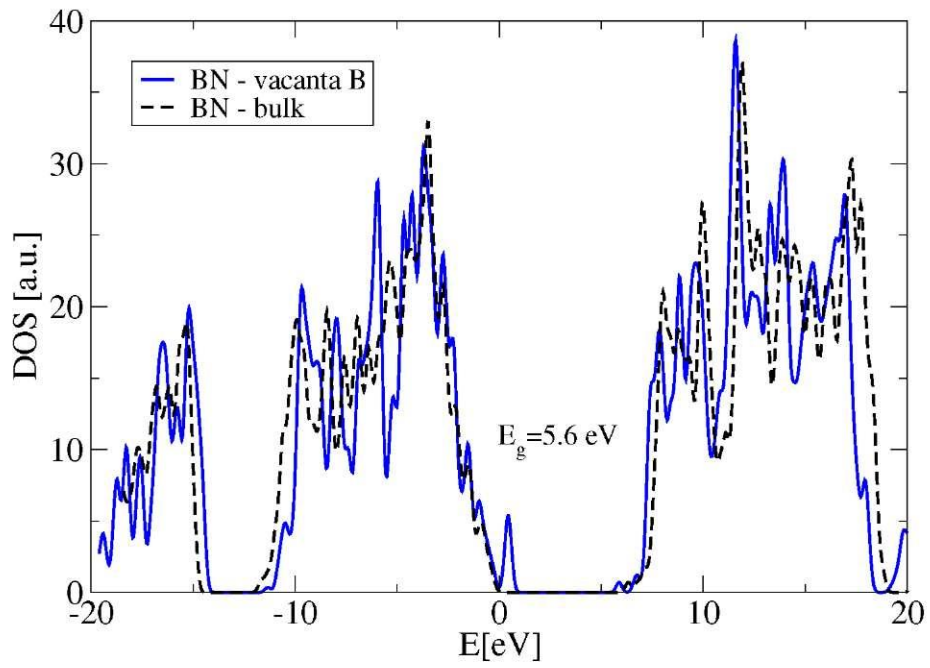
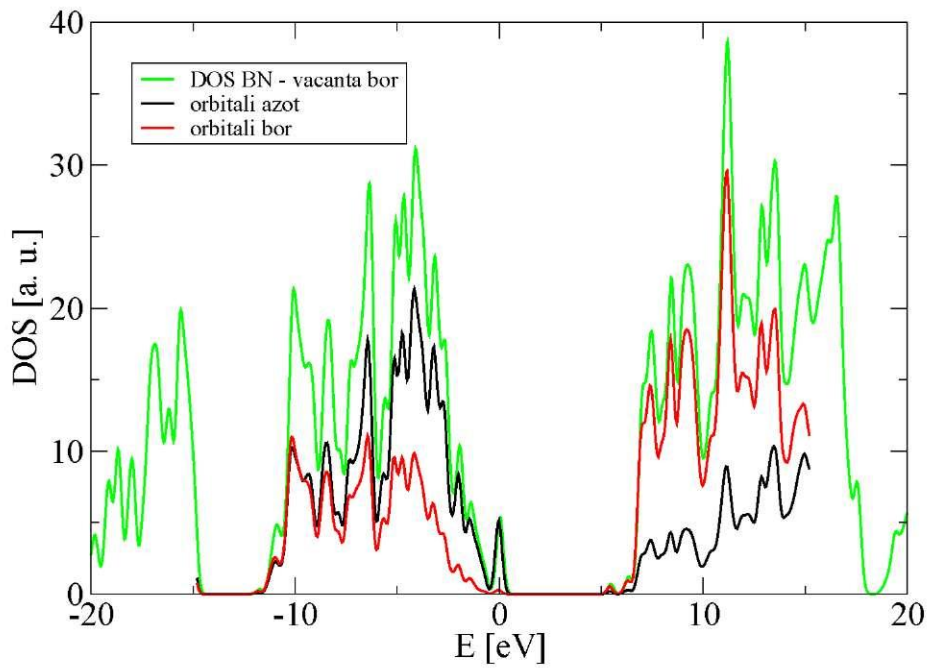
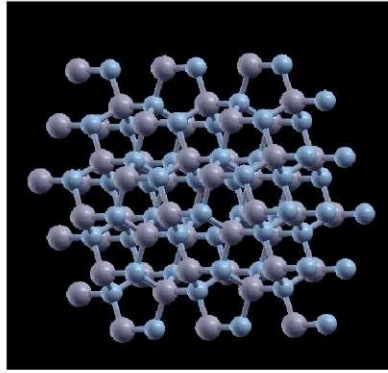


Figure 6.11: V_N in aluminium nitride after relaxation

A vacancy V_B in boron nitride (Fig. 6.12) produces a bigger split in valence band and some smaller ones in conduction band.

The states from the edge of valence band are made mostly by nitrogen orbitals and the consequence is the splitting of the valence band. Boron's orbitals are responsible for the states in the conduction band producing some new states on its edge. The defect V_B alters the top edge of valence band and for chosen size of super-cell, calculation predicts metal system. This is an artifact of the type of calculation we made because the chosen super-cell is too small. Extrapolating, we can say that this type of defect is a shallow acceptor. Because of defect V_B resulted a band gap $E_g = 5.6$ eV.

Figure 6.12: Density of states for V_B in boron nitrideFigure 6.13: Partial density of states : left- V_N in aluminium nitride, right- V_B in boron nitride

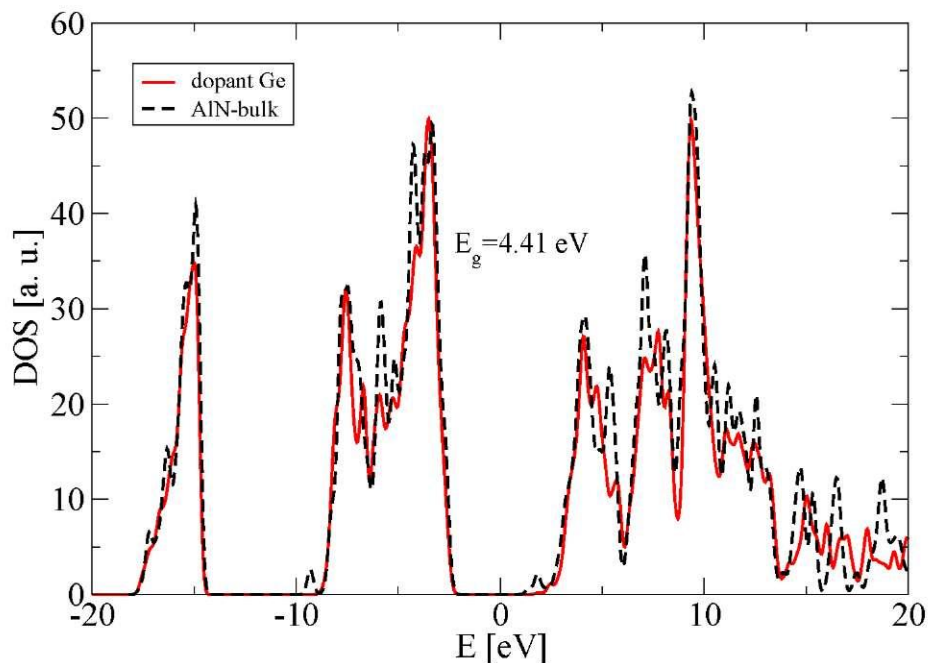
Figure 6.14: V_B in boron nitride after relaxation

6.3 Impurities

Further, we studied the effects introduced by impurities: the case of aluminium nitride with a germanium atom substituting an aluminium one I_{Ge} and the case of boron nitride doped with carbon, having the impurity atom as boron substitutional, I_C .

If we replace one atom of aluminium with a germanium atom I_{Ge} (Fig. 6.15 and 6.16) we observe the fact that on the edge of conduction band appear new states. Like before orbitals from nitrogen are related to the valence band, while the aluminium and germanium produce the states in conduction band and some new states in the band gap. In this case we can assert that the defect has a donor character.

From calculation we obtained a band gap $E_g = 4.41\text{eV}$ and a Fermi level $E_F = -2.4\text{eV}$.

Figure 6.15: Density of states : left- I_{Ge} in aluminium nitride

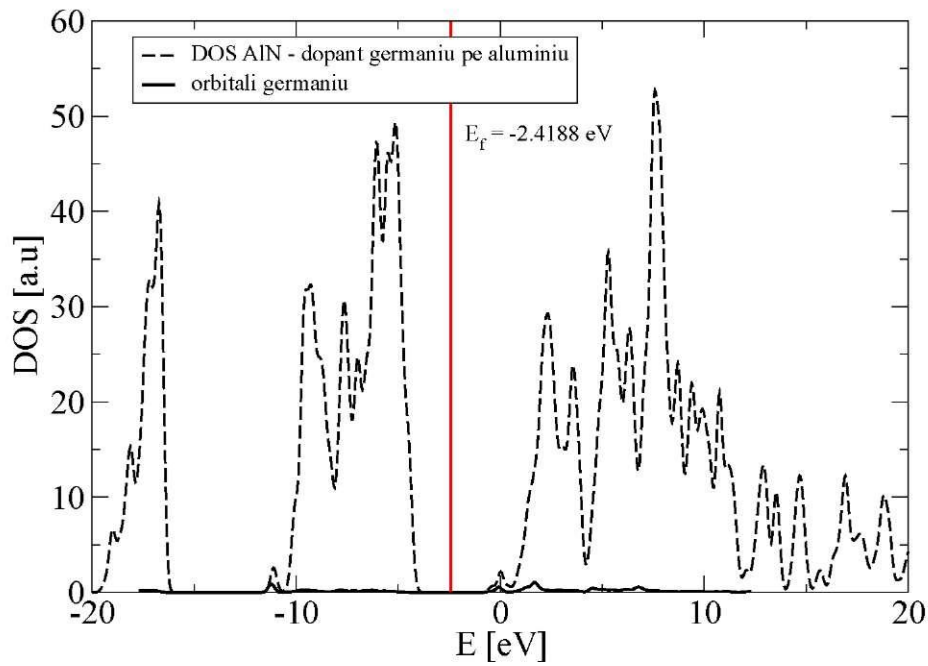


Figure 6.16: Partial density of states of I_{Ge} in aluminium nitride

For the other system, boron nitride, from Fig 6.17 and 6.18 due to the presence of I_C we observe new states inside the band gap in the energy range $[-0.83\text{eV}, 2.04\text{eV}]$. These new states are derived from boron orbitals and carbon orbitals. Most of states from conduction band derived from boron, while the states from valence band are produced both by boron and nitrogen orbitals. For this system we observed the fact that this defect has a donor character.

The band gap calculated is $E_g = 5.6\text{eV}$.

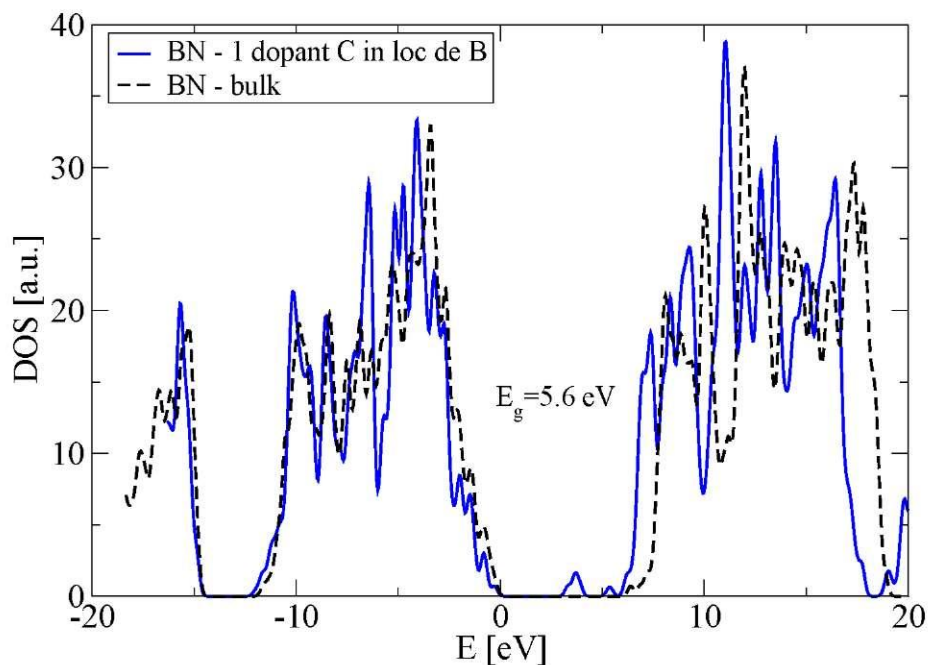


Figure 6.17: Density of states I_C in boron nitride

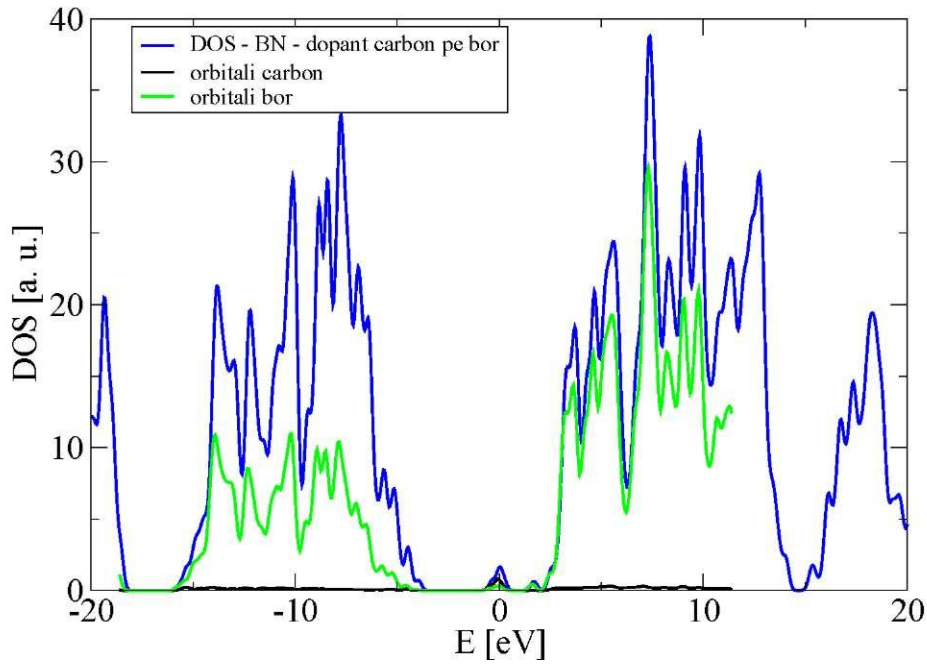


Figure 6.18: Partial density of states: left I_C in boron nitride

6.4 Complex defects

For complex defects we studied the aluminium nitride with a vacancy of nitrogen V_N and an impurity of silicon I_{Si} in a place of an aluminium atom, and the boron nitride with a vacancy of nitrogen V_N and an impurity of silicon I_{Si} in a place of a boron atom.

In Fig. 6.20 we can observe around energies with values between -1.27eV and 1.46eV new states in band gap. These states come from both nitrogen and silicon orbitals. The states from valence band come largely from nitrogen orbitals. We notice that this association of defects creates an amphoteric defect which give rise to deep donor levels and deep acceptor levels.

In this case the band gap is $E_g = 3.3003\text{eV}$.

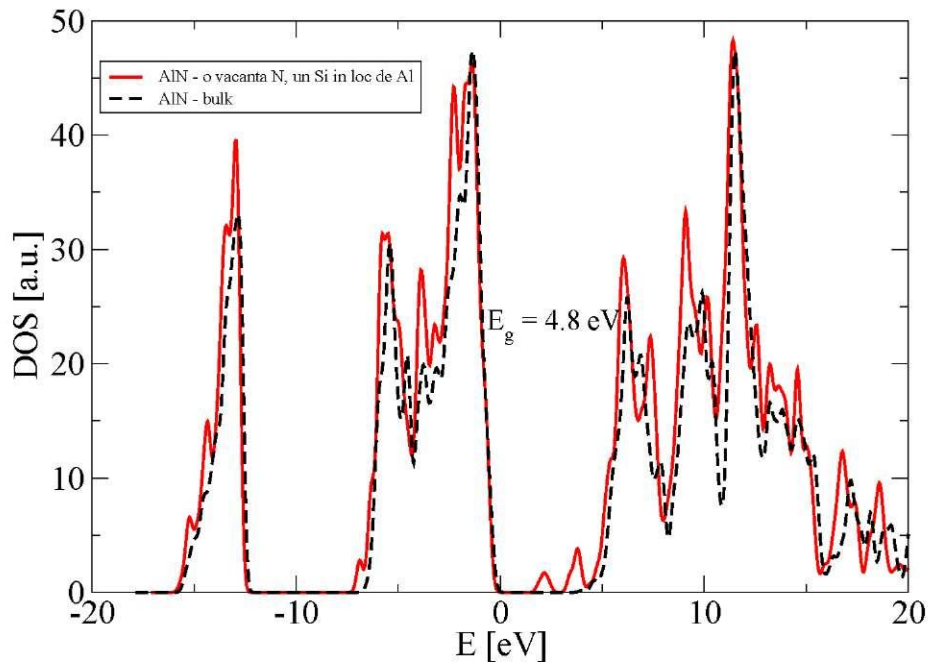


Figure 6.19: Complex defect in aluminium nitride - density of states

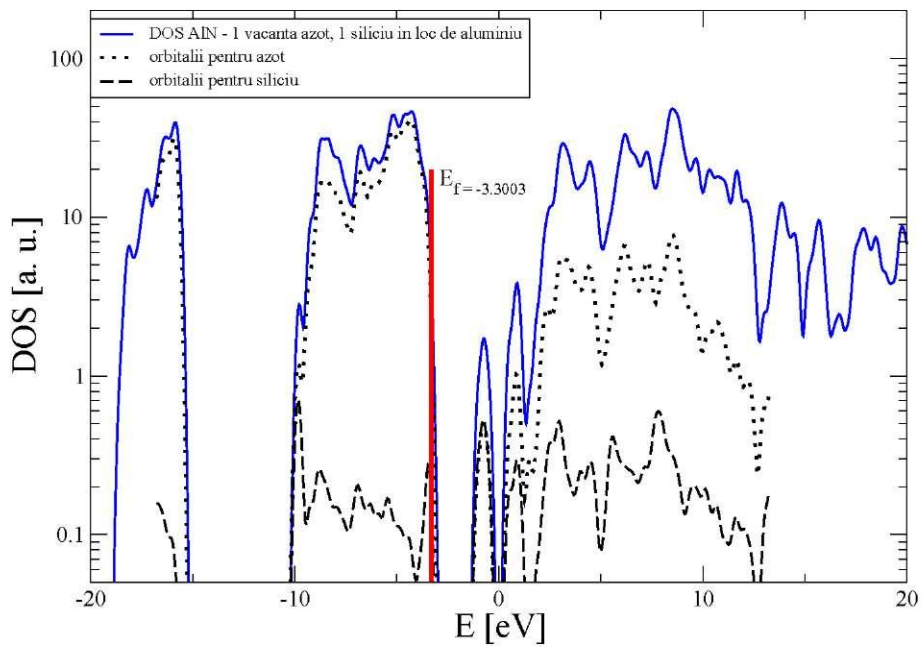


Figure 6.20: Partial density of states - complex defect in aluminium nitride

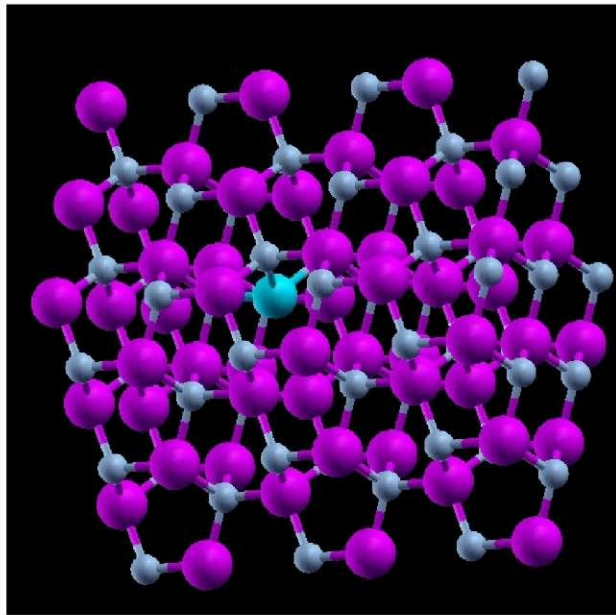


Figure 6.21: Complex defect in aluminium nitride after relaxation

The same defect was studied for boron nitride. In this structure we notice new bands inside the band gap of the ideal bulk material, states generated mainly by boron and silicon orbitals. New donor and acceptor levels appear, but the splitting between donor and acceptor centers is higher compared to AlN system. The silicon orbitals and boron orbitals produce new states in the middle of the band gap and boron and nitrogen orbitals produce the states at the edge of the conduction band.

From calculation results a band gap $E_g = 6.1 \text{ eV}$.

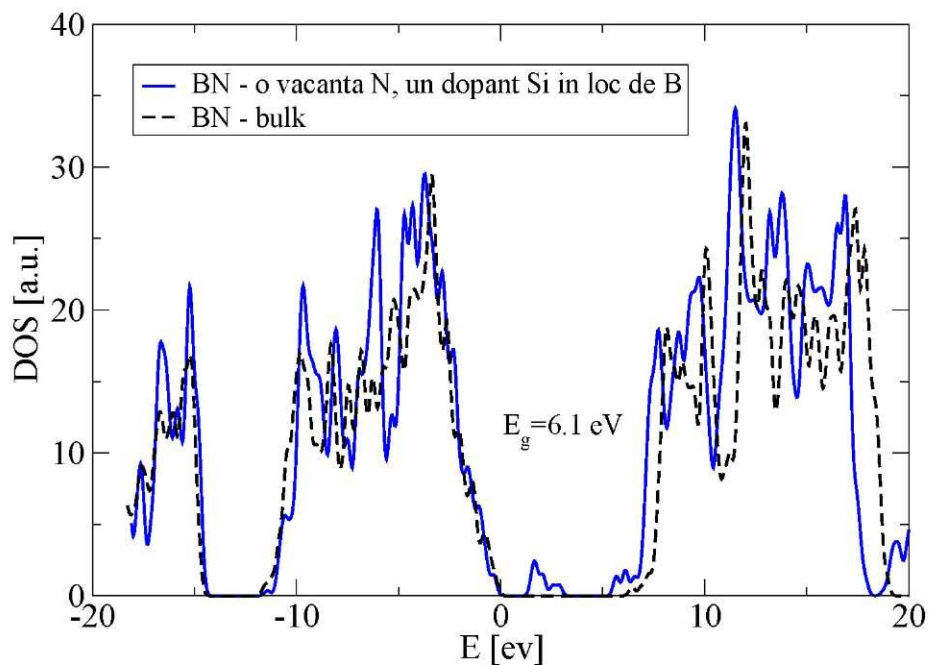


Figure 6.22: Density of states - complex defect in boron nitride

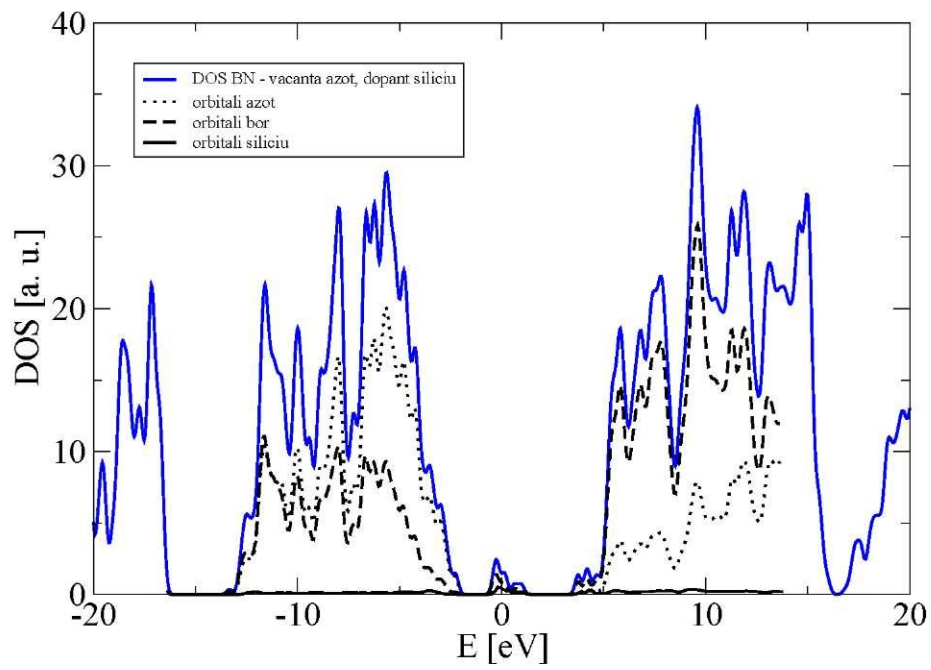


Figure 6.23: Partial density of states - complex defect in boron nitride

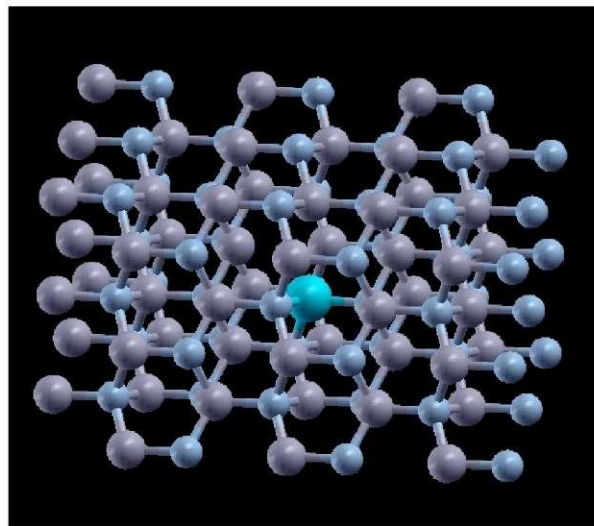


Figure 6.24: Complex defect in boron nitride after relaxation

Chapter 7

Conclusions

We indicated the influence of different types of defects on the band structure of two wide band gap wurtzite semiconductors, namely, boron nitride and aluminium nitride. The DFT calculation results made so far showed that :

- in case of aluminium nitride system, germanium is an efficient donor and silicon dopant together with a nitrogen vacancies give rise to new donor and acceptor levels; we established the positions of these energy levels

- in case of boron nitride system, carbon is an efficient donor and silicon dopant together with nitrogen vacancies also give rise to donor and acceptor levels, but in this case the splitting between two centers, donor and acceptor, is higher.

We identified the nature of the valence and conduction bands, as well as of the different impurity levels in terms of *s* and *p* orbitals. These yield direct conclusions over the allowed and forbidden radiative transitions.

From the DFT calculations that were undertaken one can extract the formation energies in the different systems and therefore one can establish which type of defect is more likely or whether a certain atomic species constitutes an efficient dopant as a donor or an acceptor.

For the future we intend to study other more complex types of defects in aluminium nitride and boron nitride and to calculate the formation energy of such defects.

Chapter 8

Personal thanks

I would like to thank to the people that helped me during last years : to Conf. Dr. Lucian ION and Dr. Alexandru G. NEMNES, for the given support, for all the time they spent offering explanation and good advices; to Prof Dr. Stefan ANTOHIE, the head of the MDEO research center for giving me the chance to make my master thesis in his research group, for all his advices and support; to all the professors from the Faculty of Physics, my colleagues; and last but not least i would like to thank to the others members of MDEO research group : Sorina IFTIMIE and Cristina BESLEAGA for their support and friendship.

Bibliography

- [1] Electronic Structure - Basic Theory and Practical Methods - Richard Martin
- [2] Fundamentals of Density Functional Theory - Walter Kohm
- [3] M. Lannoo, J. Bourgoin : "Point Defects in Semiconductors"-Springer Series in Solid State Sciences, pag.1-9
- [4] J.M. Soler, E. Artacho et al. 2002 J. Phys. : Condens. Matter
- [5] Kobayashi,A.,Sankey,O.F., Volz, S.M., Dow, J.D.Phys.Rev.B28 (1983)
- [6] Christensen, N.E., I. Gorezyca, Phys. Rev B 50:4397 (1994)
- [7] Xu,Yong-Nian,W.Y. Ching Phys. Rev.B 44:7787 (1991)
- [8] T. Soma, Sawaoka. A, Saito - Materials Research Bulletin (1974)
- [9] A.M. Stoneham : "Theory of Defects in Solids" - Clarendon Presee, Oxford (1975)
- [10] O. Madlung: "Introduction to Solid-State Theory" - Springer Ser, Solid-State Sci,Vol2. (1978)
- [11] R. Englman: The Jan-Teller Effect in Molecules and Solids (1972)